Diurnal and day-to-day characteristics of ambient particle mass size distributions from HR-ToF-AMS measurements at an urban site and a suburban site in Hong Kong

Berto P. Lee[1], Hao Wang[2], and Chak K. Chan[1,2*]

[1]School of Energy and Environment, City University of Hong Kong, Hong Kong, China

[2]Division of Environment, Hong Kong University of Science and Technology, Hong Kong, China

Correspondence to: Chak K. Chan (chak.k.chan@cityu.edu.hk)

Abstract. Mass concentration based particle size distributions measured by a high-resolution aerosol mass spectrometer were systematically analyzed to assess long and short-term temporal characteristics of ambient particle size distributions sampled at a typical urban environment close to emission sources and a suburban coastal site representing a regional and local pollution receptor location in Hong Kong. Measured distributions were bimodal and deconvoluted into submodes which were analyzed for day-to-day variations and diurnal variations.

Traffic and cooking emissions at the urban site contributed substantially to particle mass in both modes, while notable decreases in mass median diameters were limited to the morning rush hour. Inorganic particle components displayed varying diurnal behavior, including nocturnal nitrate formation and daytime photochemical formation evident in both modes. Suburban particle size distributions exhibited notable seasonal disparities with differing influence of local formation, particularly in spring and summer, and transport which dominated in the fall season leading to notably higher sulfate and organic accumulation mode particle concentrations. Variations in particle mixing state were evaluated by comparison of inter-species mass median diameter trends at both measurement sites. Internal mixing was prevalent in the accumulation mode in spring at the urban site, while greater frequency of time periods with external mixing of particle populations comprising different fractions of organic constituents was observed in summer. At the suburban site, sulfate and nitrate in the accumulation mode more frequently exhibited differing particle size distributions in all seasons signifying a greater extent of external mixing.

At the urban site, periods of greater submicron inorganic mass concentrations were more likely to be caused by increases in both Aitken and accumulation mode particle mass in summer, while at the suburban receptor location organic and nitrate Aitken mode particle mass contributed more regularly to higher total submicron species mass concentrations in most seasons (spring, summer and winter).

1. Introduction

Apart from mass and chemical composition, the size distribution of fine particles represents a vital physical property with important implications for human health and environmental effects of ambient aerosols (Seinfeld and Pandis, 2006). Particle size relates directly to the aerodynamic properties which govern the penetration and deposition of particles in the airways and lungs (Davidson et al., 2005) as well as the scattering and absorption of light which affect the radiative properties and hence ambient visibility (Ahlquist and Charlson, 1967;Bohren and Huffman, 1983;Charlson et al., 1991;Schwartz, 1996;Seinfeld and Pandis, 2006). Hygroscopic growth in response to changes in ambient humidity can alter particle light scattering properties (Seinfeld and Pandis, 2006;Köhler, 1936) and activation of condensation nuclei particles into cloud droplets depend on atmospheric conditions, chemical composition, mixing state as well as the size and morphology of particles (Abbatt et al., 2005;Kerminen et al., 2012;Meng et al., 2014;Westervelt et al., 2013).

Studies into the size distribution of ambient particulate matter in Hong Kong have been largely based on size-segregated filter samples (Yao et al., 2007b;Zheng et al., 2008;Zhuang et al., 1999;Huang et al., 2014;Bian et al., 2014) and measurements by electrostatic classifier instruments (Cheung et al., 2015;Yao et al., 2007a) and were hence either limited in size resolution (offline filter samples) or chemical resolution (total particle count by classification). Most measurements in Hong Kong were conducted in suburban environments. Inorganic ammonium and sulfate were mainly found in fine mode particles in condensation and droplet mode size ranges, while nitrate had strong coarse mode contributions (Zhuang et al., 1999). Seasonal differences were evident in solvent-extractable organics and trace metals which were mainly found in $PM_{0.5}$ particles in the wet season and winter whereas in fall a shift to larger particles (0.5–2.5 μm fraction) in fall indicated a possibly stronger influence of aged particle components in the transition period of the Asian monsoon (Zheng et al., 2008). Size distributions acquired by a fast mobility particle sizer at the suburban HKUST supersite were investigated more recently to study the formation and accumulation of ultrafine particles under different air flow regimes. Particle number concentration enhancements during the day were attributed to secondary formation, while evening and nighttime peaks were thought to be related to transport of aged aerosols from upwind locations. Nucleation mode particle peaks were often observed in fall and related to regional pollution influence (Cheung et al., 2015). New particle formation events at the same site occurred as single and two-stage growth processes with organics and sulfuric acid contributing mainly to first stage growth in the daytime while nighttime second stage growth was attributed to ammonium nitrate and organics. Particle size growth into the diameter range of cloud condensation nuclei (CCN) was typically only achieved with the second growth stage (Man et al., 2015).

Investigations into particle size distributions in urban areas of Hong Kong are even scarcer. Yao et al. (Yao et al., 2007a) studied the properties and behavior of particles in vehicle plumes and reported a competing process between ambient background particles and fresh soot particles in the condensation of gaseous precursors and a dependency on temperature with bimodal volume size distributions observed at lower ambient temperatures and unimodal distributions in the lower accumulation size range at higher ambient temperatures.

The Aerodyne aerosol mass spectrometer (Canagaratna et al., 2007) is widely used to determine the chemical composition of major organic and inorganic components of non-refractory submicron particulate matter ($NR\text{-}PM_1$). In contrast to most traditional aerosol sizing instruments, the AMS is capable of resolving main chemical constituents

within size distributions through analysis of particle flight times and particle ensemble mass spectra (Canagaratna et al., 2007;Jayne et al., 2000;Jimenez et al., 2003;Rupakheti et al., 2005) and thus yields valuable additional information on differences in composition of submicron particles with the gross of particle mass in the Aitken mode range (D_p ~ 10-100nm) and the accumulation mode range (D_p ~ 100-1000nm) covered by the AMS. Thus far most studies employing ambient size distribution data from aerosol mass spectrometer measurements investigated longer time period averages, i.e. campaign averages (Salcedo et al., 2006;Sun et al., 2009;Aiken et al., 2009;Huang et al., 2010;Takegawa et al., 2009;Saarikoski et al., 2012;Li et al., 2015) or specific time periods of interest (Elser et al., 2016;Lee et al., 2013). Mohr et al. separated organic particle mass size distributions by periods of dominant influence of different PMF-resolved organic aerosol factors to study the properties of mass size distributions in relation to organic aerosol composition (Mohr et al., 2012). The 3D-factorization technique is an extension of traditional AMS PMF analysis on organic aerosol allowing to obtain estimates on the size distributions of organic aerosol factors, however under the assumption that factor size distributions remain invariant over the measurement period (Ulbrich et al., 2012).

The temporal evolution of species-specific size distributions, are mostly discussed qualitatively (Drewnick et al., 2005) and only few studies have evaluated temporal trends in mass size distributions in greater detail. Particle nucleation and subsequent growth events were investigated in Pittsburgh using size data from an AMS and two SMPS as well as various gaseous pollutant instruments and meteorological information. The AMS mass size distributions were evaluated quantitatively using the time series of binned particle concentrations generated from the grouping of raw data into wider size bins to represent different stages in the particle growth process. (Zhang et al., 2004). The same method was employed to evaluate contributions of ultrafine mode and accumulation mode particles to total organic particle mass (Zhang et al., 2005) by summation of size bins in the range of 30-100 nm and 100-1000nm. The authors also explored diurnal changes in size distributions of particle species by averaging over 3h periods in the morning (6–9 am) and afternoon (1–4 pm). Sun et al. present a qualitative discussion of diurnal variations in the mass size distributions of the m/z 44, m/z 57 and derived $C_4H_9^+$ ion signals from measurements at an urban site in New York (Sun et al., 2011). Similarly, Setyan et al. examined diurnal changes in the mass size distributions of organics and sulfate qualitatively and used binned concentrations (40–120, 120–200, and 200–800) nm in their quantitative analysis to study the evolution of particle chemistry in new particle formation and growth events (Setyan et al., 2012).

In this work, we introduce a systematic approach of assessing temporal variations in AMS mass-based particle size distributions from hourly diurnal variations to 24h-average based day-to-day trends to utilize two key instrumental advantages, i.e. species segregation and high time resolution, to obtain a more detailed and quantitative understanding of the variabilities in ambient particle mass size distributions and to provide an additional dimension to standard AMS data analysis techniques. In this context, we present a detailed discussion of particle size data from HR-ToF-AMS measurements during two field campaigns in Hong Kong in both urban and suburban environments. We aim to evaluate characteristic recurrent changes in size distribution as well as longer term trends in different seasons by analyzing day-to-day variations and diurnal variations of size distributions of submicron organics, sulfate, and nitrate particle mass. The two contrasting sites represent a typical urban source environment (inner-city, roadside station)

close to primary emission sources and a suburban location (coastal, HKUST supersite) which is largely a downwind receptor of varying amounts of local urban, regional and long-range transported pollutants (Li et al., 2015;Huang et al., 2014).

2. Methodology

2.1. Field campaigns

Sampling of ambient submicron non-refractory particulate matter (NR-PM_1) was carried out using an Aerodyne HR-ToF-AMS at the HKUST air quality supersite covering four seasons between May 2011 and February 2012 (spring: 2011-05, summer: 2011-09, fall: 2011-11&12, winter: 2012-02). The HKUST supersite is located on the campus of the Hong Kong University of Science and Technology (22°20'N, 114°16'E), on the east coast of Hong Kong in a suburban area with few primary emission sources in the immediate vicinity. Sampled air was drawn from the rooftop of a pump house building at an approximate height of 25m above ground level. For detailed descriptions of the experimental setup, operating conditions, data treatment, and overall species composition we refer the reader to previous publications (Lee et al., 2013;Li et al., 2015;Li et al., 2013). A further sampling campaign took place between spring 2013 (2013-03 to 2013-05) and summer 2013 (2013-05 to 2013-07) at an inner-city urban location in the densely populated and built-up Kowloon peninsula. Measurements were conducted next to the roadside air quality monitoring station (AQMS) operated by the Environmental Protection Department (EPD) of the HKSAR Government in the Mong Kok (MK) district on a pedestrian crossing at a major road junction. Sampled air was drawn from a height of 3m above ground level. A comprehensive analysis of trends in species concentration and composition identified in this urban campaign has been presented previously (Lee et al., 2015). In both campaigns, particles were sampled through a $PM_{2.5}$ cyclone at a flow rate of 16.67 L/min into a sampling port from which 0.08 L/min was drawn by the AMS and the remainder drawn by co-sampling instruments and an auxiliary pump. Sample air for the AMS passed through a 1m long diffusion dryer (BMI, San Francisco CA, USA) filled with silica gel to remove bulk gas- and particle-phase water. Additional data from various collocated instruments including meteorological data (wind, temperature, relative humidity, solar irradiation), volatile organic compounds (VOCs) and standard trace gases such as NO_x, SO_2, and O_3 were available.

AMS data were treated according to general AMS data treatment principles (DeCarlo et al., 2006;Jimenez et al., 2003) with standard software packages (SQUIRREL, PIKA). Analysis of the unit-mass resolution mass spectra yielded non-refractory submicron particle species concentrations of major inorganic constituents (SO4, NO3, NH4, Chl) and total organics at a base time resolution of 10 min. Positive Matrix Factorization (PMF) was used to deconvolute high-resolution organic mass spectra acquired at 10 min time resolution following recommended PMF guidelines for AMS data (Zhang et al., 2011) with the AMS PMF analysis toolkit (Ulbrich et al., 2009). At the urban Mong Kok site, six organic aerosol (OA) factors were identified encompassing three secondary organic aerosol (SOA) and three primary organic aerosol (POA) factors of which one was attributed to traffic emissions and two to cooking activities (Lee et al., 2015). Similarly, four factors were obtained from analysis of the urban HKUST site dataset with two SOA factors

and two POA factors, related to traffic and cooking respectively (Li et al., 2015). Further details on the treatment of AMS size distribution data from both sampling campaigns are provided in the following section.

2.2. Data acquisition and treatment

In both campaigns, mass concentration based size distributions in terms of vacuum-aerodynamic particle diameter ($dM/d\log D_{va}$) were established by joint acquisition of particle time-of-flight (PToF) measurements and unit mass resolution mass spectra (V-mode) with alternation between modes every 20s for 30 cycles amounting to 5 min of total sampling time. High-resolution mass spectra were acquired for the following 5 min, and thus the overall raw data time resolution for each mode was equal to 10 min. The total particle mass measured in the PToF mode was normalized to the V-mode mass concentration of the same time step. Daily size distributions were generated by averaging over 24h periods (from 0:00 to 23:59). Hourly diurnal size distributions were reconstructed by grouping size distributions within the same hour of the day and establishing representative size distributions based on average, median, 25^{th} and 75^{th} percentile concentration values of each size bin (*referred to as size distribution sets hereinafter*).

At both sampling sites, the seasonally averaged AMS size distributions were bimodal (Lee et al., 2013, 2015;Li et al., 2015) with similar distributions having been observed in other AMS field studies in various parts of the world. (Zhang et al., 2014;Sun et al., 2011;Huang et al., 2011;Aiken et al., 2009;Zhang et al., 2005;Crippa et al., 2013;Docherty et al., 2011;Mohr et al., 2012). Multimodality of size distributions is typical for environments where different sources or formation processes of particles play a role and accordingly such distributions can also be represented as sums of discrete lognormal distributions of the respective constituting submodes (John, 2011).

The measured bimodal size distributions in this work were deconvoluted by fitting two log-normal distributed modes, including one closer to the Aitken size range (*mode diameter ~100nm*) and one in the accumulation size range (*mode diameter ~500nm*) employing the Levenberg-Marquardt algorithm (Gill et al., 1981) as a non-linear least squares fit, to evaluate differences in trends and formation or transformation processes in the two size regimes. An example of a size distribution fit and associated parameters is depicted in Figure D1 in the Supporting Material. Additional fit residual analyses were carried out in cases where the Aitken mode only accounted for small parts of (<10%) of the total particle mass and uncertainties in integrated mode particle mass from the peak fitting were examined for all size distributions. Details are presented in Section B of the Supporting Material. The smaller mode typically exhibited mode diameters in the range of 100-200 nm (D_{va}) and is thus in the transition region between Aitken and lower accumulation mode. For a clearer distinction from the larger mode which unambiguously belonged to the accumulation size range, we opt to refer to the small mode as *Aitken mode* in this work. Mode diameter (*i.e.* mass median diameter, MMD), curve width (*i.e.* geometric standard deviation, GSD) and curve area (*equivalent to particle mass concentration within the mode*) are sufficient parameters to completely describe a lognormal distribution and these key variables are used in the following analysis on trends in the fitted species-specific size distributions of organics, nitrate, and sulfate from both HR-AMS sampling campaigns in Hong Kong. Particle diameters are discussed in terms of vacuum-aerodynamic diameter, with detailed discussions on properties and relationships to other size metrics available elsewhere (DeCarlo et al., 2004;Slowik et al., 2004). Further details on procedures of PToF data

acquisition and size distribution averaging can be found in the Supporting Material in Section A and B respectively. The sequence of main data treatment and analysis steps is shown in Figure 1.

The transmission efficiency of the AMS aerodynamic lens is known to fall off below ~100nm and beyond ~550 nm of vacuum-aerodynamic diameter (Liu et al., 2007;Takegawa et al., 2009;Zhang et al., 2004;Bahreini et al., 2008;Williams et al., 2013;Knote et al., 2011) and may bias measured particle mass and mode diameters, particularly in the accumulation mode towards lower values if significant particle mass fractions fall in the size region of D_{va} > 550 nm. In the Aitken mode range, the effect of limited lens transmission is expected to be less substantial as particle volume (and hence particle mass) of Aitken mode particles are much smaller. We discuss the effects of lens transmission briefly in section 3.4. Delayed vaporization of particle components, e.g. under high mass loadings, can lead to small shifts towards larger mode diameters in AMS size distributions (Docherty et al., 2015) and enhanced tails in the size distributions (Cross et al., 2009), which may lead to larger fit residuals at the trailing edges. Generally, the discussion of size distributions in this work should be viewed in the context of the instrumental capabilities and previously mentioned limitations of aerosol mass spectrometry. Therefore, the resolved Aitken and accumulation modes in this work reflect the apparent Aitken and accumulation modes within AMS measurable particle mass size distributions.

semi-volatile constituents towards the particle-phase. We expect these volatility effects to be a main contributing factor, as sampling took place in direct vicinity of the emission source, i.e. next to the road and thus potential impacts of physical effects such as enhanced near-ground mixing and dispersion through thermally induced convection in summer are expected to be of minor influence. Considering the previously discussed estimated traffic contributions during the rush hour, the seasonal difference in mass concentration was much more pronounced in the Aitken mode (-67%, 0.6 $\mu g/m^3$) than the accumulation mode (-12%, 0.2 $\mu g/m^3$), consistent with the expected stronger impact of reduced particle nucleation and reduced condensation of semi-volatile exhaust components on fresher, smaller particles in the warmer season.

Comparing different size distribution sets (Figure D6 in the Supporting Material), the average concentration set in summer yielded notably larger resolved mass median diameters in both modes and greater Aitken mode mass compared to the median, 25^{th}, and 75^{th} percentile concentration sets. This indicates a strong influence of extreme values (i.e. time periods with both larger particle size and larger particle mass concentrations) and thus greater variability in size distributions in the warmer season caused by specific high and low concentration events such as photochemical episodes and precipitation, evident in the greater relative span of organic mass concentrations in summer (See Table C5 in the Supporting Material: ratio of 10th and 90th percentile to median concentration in NR-PM_1). In spring, such events masked the diurnal processes to a lesser extent and with consequently greater consistency across different size distribution sets.

Sulfate

Although variations of total submicron sulfate mass concentrations with time of day were generally subtle, distinct trends were notable in MMDs and integrated mode mass concentrations in both Aitken and accumulation mode.

Generally, Aitken mode MMDs were 20% larger in spring (180nm) than in summer (150nm). While in spring fluctuations in Aitken mode MMDs were small throughout the day within a narrow range of +/- 10nm and without apparent regular features, the summertime diurnal variation exhibited a well-defined broad daytime peak with a shift to ~15nm larger particle diameters. A matching trend was evident in the accumulation mode where MMDs increased by ~20nm in summer. Conversely, in spring, a conspicuous nighttime peak in accumulation mode MMDs was observed in the low traffic period between 01:00 and 07:00 which tracked closely with the diurnal variation of O_3 which peaked in the same period with the reduction of the NO_x titration effects at low nighttime traffic volumes. While particulate sulfate production during the day can be achieved through both homogeneous gas-phase oxidation of SO_2 by the OH radical as well as heterogeneous oxidation of SO_2 by dissolved H_2O_2 or O_3 (Seinfeld and Pandis, 2006), nighttime production is limited to the non-photochemical heterogeneous pathway. The apparent increase in accumulation mode particle size was also associated with an increase of integrated submode particle mass by ~0.7 $\mu g/m^3$ and thus suggests the possibility of heterogeneous SO_2 oxidation by residual ozone in the cooler and more humid spring season as a local source of particulate sulfate. In the warmer and drier summer season, no corresponding trend was apparent in either accumulation mode MMD or integrated mode concentration. The small magnitude of additionally produced sulfate (< 1 $\mu g/m^3$) in spring renders the nighttime production a minor source of particulate sulfate however and affirms that the bulk of the accumulation mode sulfate burden at the urban roadside still originated

Figure 4. Diurnal variations of mode diameter (MMD), integrated mode mass concentration and width of the Aitken mode (*lighter color*) and accumulation mode (*darker color*) from bimodal peak fits of the bin-median reconstructed size distributions at the suburban HKUST site and V-mode AMS species concentrations (line with shaded background) for organics, nitrate and sulfate (left to right) in (a) Spring 2011, (b) Summer 2011, (c) Fall 2011 and (d) Winter 2012; The right-most panel depicts the median diurnal variations of relevant gas-phase pollutants (O3, CO, NOx, SO2) measured at the same site.

3.1.2. Suburban coastal NR-PM_1

The suburban HKUST site as a downwind receptor of urban and regional pollution was generally dominated by sulfate and oxygenated secondary organic aerosol (SOA) components and much lower fractions of primary organic constituents, which combined typically made up less than a quarter of total organics (Li et al., 2015). Trends in the species segregated particle size distributions are discussed analogously to section 3.1.1., with Figure 4 illustrating the diurnal trends of the fitting parameters (MMD, integrated mode mass, geometric standard deviation) for organics, sulfate, and nitrate at the suburban HKUST site.

Organics

There were significant seasonal differences with larger fractions (Figure 3b) and concentrations (Figure 5c) of Aitken mode mass in total organic submicron particle mass in spring and summer compared to fall and winter, indicating greater influence of closer-ranged formation sources in the warmer season. Springtime integrated Aitken mode mass concentrations (~0.8 $\mu g/m^3$) were twice as high as those in winter (~0.4 $\mu g/m^3$). In the accumulation mode, highest particle mass loadings were observed in fall (5 $\mu g/m^3$) and lowest loadings in spring (3 $\mu g/m^3$) following the frequency pattern of continental air mass influence (Figure D12 in the Supporting Material) in each season indicating continental transport of particulate mass or gas-phase precursors. Lowest mass concentrations in the Aitken mode typically occurred in the night hours (00:00 – 05:00) in a range of 0.3 – 0.5 $\mu g/m^3$ in spring, summer, and winter, while in fall mass loadings of 0.7 - 0.8 $\mu g/m^3$ were reached. Diurnal changes were least pronounced in winter with largely constant integrated Aitken mode particle concentrations. In the remaining seasons, varying degrees of daytime changes were apparent with a general increase around 06:00, likely owing to citybound commuter traffic from surrounding roads to the west of the sampling site at 1-2km of lateral distance. This also led to a modest increase in particle polydispersity with a discernible widening of the Aitken mode size distributions (*black solid line, lowest panels in* Figure 3). Daily maxima in spring, summer and fall were reached in the early evening (~21:00) with marked differences in absolute mass concentrations depending on the respective season, from a summer time low of 0.8 $\mu g/m^3$ to a fall season high of 1.4 $\mu g/m^3$. Mass median diameters in the Aitken mode were smaller in the night hours and displayed subtle increments during the day in the range of 10-20 nm reaching their maximum typically in the late afternoon, except for the fall season when mass median diameters displayed very little variation with time of day.

Total particle mass in the accumulation mode in spring and summer reached minima during the night hours (2 $\mu g/m^3$) and maxima (3 $\mu g/m^3$) around noon, remaining stable in the daylight hours thereafter. MMDs increased notably from 440nm at night to 510nm during the day in spring, while in summer a morning rise by ~30nm from 530nm to 560nm was obvious between 06:00 and 10:00 and coincided with the morning rush hour and the associated early morning

peak of NO_x and an otherwise stable mode diameter of 530nm for the rest of the day. In fall, the increase in accumulation mode organic mass occurred much earlier, starting in the dark hours at 04:00, with a corresponding trend also evident for nitrate but absent for sulfate, indicating a common source of these organic and nitrate enriched particles. Nighttime MMDs for organics were generally larger (540nm) and decreased to a minimum of 510nm in the early afternoon accompanied by a slight widening of the distribution. In winter, mass concentrations decreased appreciably in the early morning hours and started to increase only beyond 10:00. In the colder seasons (fall, winter), a similar concentration pattern was also observed for gas-phase SO_2 which is considered as a largely regional pollutant with few distinct local sources (Yuan et al., 2013), indicating that changes in boundary layer and mixing with regional background were likely the more dominant processes in winter.

Sulfate

Aitken mode sulfate mass concentrations peaked in the afternoon from spring throughout fall with maximum concentrations reached progressively later in the afternoon (14:00 in spring; 16:00 in fall). Nominal concentrations were highest in spring and summer (0.5-0.6 $\mu g/m^3$), slightly lower in fall (0.4 $\mu g/m^3$) and reached the lowest levels in winter (0.1 $\mu g/m^3$). In addition to the afternoon peak, a conspicuous early morning peak of similar magnitude was evident in spring between 02:00 and 06:00. A greater proportion of southerly winds was evident in said time period compared to the overall seasonal wind frequency distribution (Figure D13a in the Supporting Material) and may indicate transport of sulfate from marine sources in the southern parts of Hong Kong. Diurnal variations in MMDs and GSDs were generally small and without obvious regular trends. Nominal mass median diameters were significantly lower in winter (~170nm) compared to spring and fall (~190nm) and summer (~210nm).

Trends in accumulation mode particle mass were more pronounced. In spring, a shallow concentration valley during the late evening and night hours (20:00 to 03:00) with minimum concentrations of 5 $\mu g/m^3$ was apparent, while daytime concentrations stayed largely invariant at 6 $\mu g/m^3$. The MMDs followed a similar variation with a minimum mode diameter around 550nm in the early hours of the day and slightly larger daytime MMDs around 570nm. Nominal concentrations were larger in summer with a nighttime valley concentration of 7 $\mu g/m^3$ and a well-pronounced broad day peak with a maximum of 9.5 $\mu g/m^3$ in the early afternoon (14:00-15:00). A prior additional morning peak occurred between 04:00 and 10:00 with particle mass concentrations reaching 8.5 $\mu g/m^3$ related to a consistent north-easterly morning wind pattern (Figure D13b in the Supporting Material) and likely associated with transport from north-easterly coastal regions or nighttime fisheries related maritime traffic. The diurnal trend in mass median diameter was similar to that in spring with a night minimum of 570nm and day maximum of 590nm.

In fall, accumulation mode characteristics showed no significant diurnal variability, with a largely stable integrated particle mass of 6 $\mu g/m^3$ and only subtle MMD changes (585nm at night; 575nm during the day). In winter, two concentration dips with reductions by ~0.5 $\mu g/m^3$ between 06:00 and 10:00 and between 18:00 and 22:00 were evident, while MMDs increased during the day between 10:00 and 15:00 from 520nm, peaking at a size of 540nm.

Nitrate

Nitrate particle mass in the Aitken mode was generally small from spring throughout fall amounting to 0.01 - 0.06

μg/m^3. Winter time concentrations were larger in a range of 0.06 - 0.08 μg/m^3 during the day and 0.10 - 0.12 μg/m^3 in the late evening hours. The latter evening peak centered around 21:00 was evident in most seasons (except spring) and accounted for 12-23% (0.1-0.25 μg/m^3) of total daily Aitken mode nitrate mass burden. Similar to the urban roadside location, these nighttime nitrate peaks coincided with the peak period of organic cooking aerosol concentrations (Figure D14 in the Supporting Material), which were however significantly smaller at the suburban measurement site and mainly attributed to the operation of an on-campus student canteen (Li et al., 2015). Trends in mass median diameters varied between seasons with no discernible trend in winter, a subtle decreasing trend with time of day in spring and broad daytime diameter increases in summer and fall. Solar irradiation in these two seasons was comparatively high (Figure D10b-c in the Supporting Material) indicating that photochemical nitrate production in the Aitken mode may have led to this observed growth in particle size.

Integrated particle mass concentrations in the accumulation mode only exhibited subtle variations from spring throughout fall, with essentially constant diurnal concentrations in spring, a subtle daytime peak in summer which accounted for ~ 15% of total daily accumulation mode nitrate (corresponding to 0.7 μg/m^3) and a conspicuous morning peak between 04:00 and 10:00 in fall accounting for ~ 5% of total daily accumulation mode nitrate (corresponding to 0.5 μg/m^3). Clearer seasonal differences were evident in the trends of MMDs. In spring, MMDs decreased appreciably over the late evening hours (21:00-0:00) with a concurrent widening of the size distribution (increase in GSD). In summer, accumulation mode diameters decreased during the day by ~40nm with a similar trend in accumulation mode organics. Winter time MMDs exhibited a more complex pattern with larger mode diameters in the early hours (04:00 – 10:00) and during the noon-time, and a late-afternoon dip leading to larger spread of intra-day mode diameters ranging from 510nm to 570nm.

In comparison to the urban roadside measurements, diurnal particle size characteristics and mass concentrations in the Aitken and accumulation mode were much more variable for all investigated species at the suburban HKUST site, indicating that longer time scale processes and irregular events (transport patterns, local meteorology) were probably more important in governing particle size distribution characteristics than diurnal processes.

3.2. Day-to-day size distributions and seasonal averages

To evaluate the evolution of particle size distributions within seasons, average species-specific size distributions were generated by averaging raw distributions over 24h periods (between 0:00 and 23:59). There was clear long-term variability in both resolved Aitken and accumulation mode MMDs and integrated submode particle mass concentrations for all species (Figures D15-16 in the Supporting Material) and overall seasonal differences which have been briefly addressed in the discussion of the diurnal size distribution variations between seasons. Figure 5 depicts the overall average values for all daily fitted MMDs and integrated particle mass concentrations in both the Aitken and accumulation mode at the suburban HKUST and urban MK sites.

3.2.1. Seasonal trends

For the MK roadside station, particle mode diameters were generally larger in spring than in summer for all three investigated species, but with clear differences in the magnitude of changes among individual species. In the Aitken mode, organics and sulfate displayed a moderate decrease in mode diameter from spring to summer by 7-8% each, while nitrate saw a more significant decrease by 25% from spring to summer. In contrast, accumulation mode MMDs for organics exhibited only a subtle decrease by 5% and more substantial decreases for sulfate and nitrate by 20-22% each. Total Aitken mode particle mass decreases varied strongly: -15% for organics, -36% for sulfate and -67% for nitrate. In the accumulation mode, organics and sulfate exhibited similar relative decreases by 40-46%, while nitrate particle mass reduced drastically by 85%.

At the suburban HKUST site, Aitken mode MMDs of nitrate and organics decreased with the progression of seasons from spring to winter with highest mode diameters observed in spring and summer and appreciable decreases in winter by -9% for nitrate and -25% for organics compared to the warmer seasons. Sulfate displayed a similar winter time decrease in MMD (-15%) and an increase of similar magnitude in the summer season (+13%) compared to spring and fall. Variations in sulfate and organic accumulation mode diameters were minor between spring and fall, while wintertime MMDs were 7-12% lower. Nitrate exhibited an overall higher variability in mass median diameters in the accumulation mode in spring (larger standard deviation) and with on average 10% lower MMDs compared to other seasons. In line with the reduction in Aitken mode MMDs in winter, the integrated Aitken mode particle mass decreased as well, by -16% for organics and almost -75% for sulfate, whereas nitrate contributions remained largely stable throughout the seasons. Organic accumulation mode particle mass was significantly higher in the fall and winter season by factors of 1.6 – 2. Diurnal variations in the degree of oxygenation were least pronounced in these seasons (Li et al., 2015) suggesting that influence of transport in autumn and winter likely dominated over local formation, thus exerting greater effects on particle mass in the larger size mode. Particulate nitrate concentrations were generally low in the accumulation mode from spring through fall, but increased sharply in winter by factors of 3 – 4. Sulfate accumulation mode mass concentrations remained more stable but saw significant summer time enhancements by ~30% likely due to photochemical activity which also led to high concentrations of Ox and a higher degree of oxygenation of organic aerosol among the four seasons (Li et al., 2015).

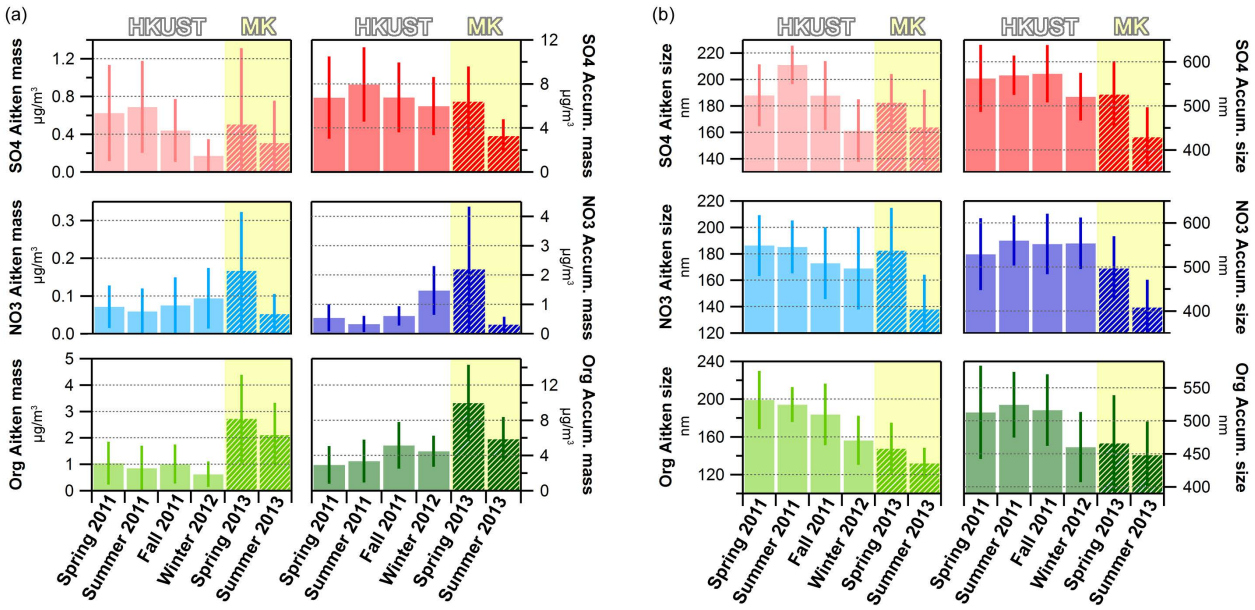

Figure 5. Average and standard deviation of daily fit values of Aitken and accumulation mode particle mass and mass median diameters at the suburban HKUST site (*solid bars*) and urban MK site (*hashed bars*). The integrated particle mass is depicted in (a) for the Aitken mode (*left panels*) and for the accumulation mode (*right panels*) for sulfate, nitrate, and organics respectively. The mass median diameter is depicted in (b) for the Aitken mode (*left panels*) and for the accumulation mode (*right panels*) for sulfate, nitrate and organics respectively.

Large particles contribute more to particle volume and hence particle mass. Correspondingly, the total submicron concentration of a given species is typically governed by changes in the accumulation mode particle mass and accordingly observed correlation values between integrated accumulation mode particle mass and individual NR-PM_1 species mass concentrations were generally high (R_{pr}>0.90) at both measurement sites (Figure D17 in the Supporting Material). This applied to both measurement sites regardless of the season. Aitken mode trends were less akin. At the urban roadside station, neither sulfate nor nitrate particle mass in the Aitken mode notably correlated with the respective total submicron species mass concentration in spring (all R_{pr}≤0.20), whereas in summer correlations were more significant with R_{pr}=0.51 for sulfate and R_{pr}=0.80 for nitrate. This signifies that periods of greater species mass concentrations were more likely to be caused by increases in both Aitken and accumulation mode particle mass indicating that particle formation and growth affecting smaller particles was more likely to occur in the warmer season. For organics, Aitken mode particle mass and submicron species mass correlated only weakly (R_{pr} = 0.26 in spring and R_{pr} = 0.38 in summer), i.e. each organic particle submode was governed by largely different dominant sources or formation processes in both seasons at the roadside.

At the suburban background site, Aitken mode particle mass for sulfate showed little correlation with total submicron sulfate concentration (R_{pr}≤0.10) apart from the spring season (R_{pr}=0.36) where more frequent wet and foggy conditions may have facilitated sulfate formation in both size modes. For organics and nitrate significantly larger correlation coefficients of submode particle mass to total species concentration ($0.5 \leq R_{pr} \leq 0.7$) were observed in most seasons (spring, summer, winter) indicating significant influence of local or regional formation processes on

543 organic and nitrate Aitken mode particulate mass at the suburban receptor location. In the fall season, much weaker
544 correlations ($0.2 \leq R_{pr} \leq 0.4$) were likely caused by the dominance of continental air mass influence (Figure D12c in
545 the Supporting Material) and greater influence of aged accumulation mode particles on total submicron nitrate mass
546 concentrations.

547 **3.2.2. Inferred changes in mixing state**

548 Shifts in mixing state of ambient particles can be inferred from the inter-species analysis of mass median diameters.
549 Close nominal agreement (i.e. diameter ratios close to 1) infer that different species were distributed similarly across
550 the particle size range which thus most likely represents a largely internally mixed particle population, while the spread
551 of data (correlation coefficient) indicates the temporal homogeneity or divergence of resolved mode diameters. A
552 hypothetically perfectly internally mixed particle population over the whole sampling period would, therefore, yield
553 MMD ratios and Pearson's R values of 1 between species, while larger or smaller values are indicative of a greater
554 frequency of heterogeneous (i.e. more externally mixed) particle populations (Figure 6).
555 At the urban Mong Kok site, changes in accumulation mode mass median diameters for nitrate and sulfate followed
556 similar trends (R_{pr} = 0.88-0.89) and with diameter ratios close to 1 (0.94–0.95) Similarly, fitted accumulation mode
557 diameters of organic constituents predominantly followed that of sulfate in spring nominally (diameter ratio 0.88) and
558 temporally (R_{pr} = 0.80). The nominal agreement of organic and sulfate accumulation mode diameters persisted
559 (diameter ratio 1.03) overall in summer, however, there was significantly more temporal divergence (R_{pr} = 0.65)
560 indicating a greater frequency of time periods with external mixing of particle populations comprising different
561 fractions of organic constituents.
562 External mixing is more prevalent for freshly formed smaller particles which have typically undergone less
563 condensational growth, coagulation or aqueous-phase reactions. Indeed, the correlation coefficients of both nitrate
564 and organic Aitken mode MMDs with respect to sulfate were notably lower (0.50 and 0.62) indicating frequent periods
565 of particle populations with different species prevailing in different size regions within the Aitken mode.
566 Sulfate and nitrate were still more likely to occur internally mixed in the Aitken mode in spring with similar diameters
567 (nitrate to sulfate MMD ratio = 1.00), while organic Aitken mode MMDs were consistently lower, indicating greater
568 fractions of organic dominated particles towards the lower end and more inorganic dominated particles towards the
569 upper end of the fitted Aitken mode.
570 In summer, both nitrate and organic MMDs tended to be lower than those of sulfate (diameter ratios of 0.79 – 0.83)
571 but similar to each other, thus implying a shift to externally mixed populations of more nitrate and organic enhanced
572 and internally mixed smaller Aitken mode particles and sulfate dominated larger Aitken mode particles.
573 At the suburban HKUST site, accumulation mode MMDs of both nitrate and organics were generally quite similar to
574 those of sulfate with diameter ratios of 0.88 – 1.06. Compared to the urban site, correlation coefficients of nitrate and
575 sulfate were consistently lower (0.54 – 0.67) indicating a much greater frequency of time periods where sulfate and
576 nitrate dominated particles in the accumulation exhibited significantly different particle size distributions.

In winter, organic MMDs were consistently lower than those of sulfate and nitrate indicating a greater proportion of externally mixed particle populations with organics enriched particles in the lower accumulation size range and inorganic dominated particles in the larger accumulation size range. The least variability in particle size was observed in the summer season where MMDs in both Aitken and accumulation mode displayed variations in relatively narrow ranges between 200-250nm and 500-700nm, whereas in the remaining seasons time periods with particle populations of lower MMD were more frequent, extending to MMDs as low as 100nm in the Aitken mode and 300nm in the accumulation mode.

In the Aitken mode, mass median diameters overall were quite similar across species, with diameter ratios of organic and nitrate distributions to those of sulfate in the range of 0.87 – 1.06, indicating that they generally covered a similar size range. The temporal agreement was highly variable with correlation coefficients (R_{pr}) spanning from 0.21 to 0.75 indicating that Aitken mode particle populations at the suburban site were generally more diverse and likely influenced by a greater range of particle formation and growth mechanisms compared to the urban Mong Kok site.

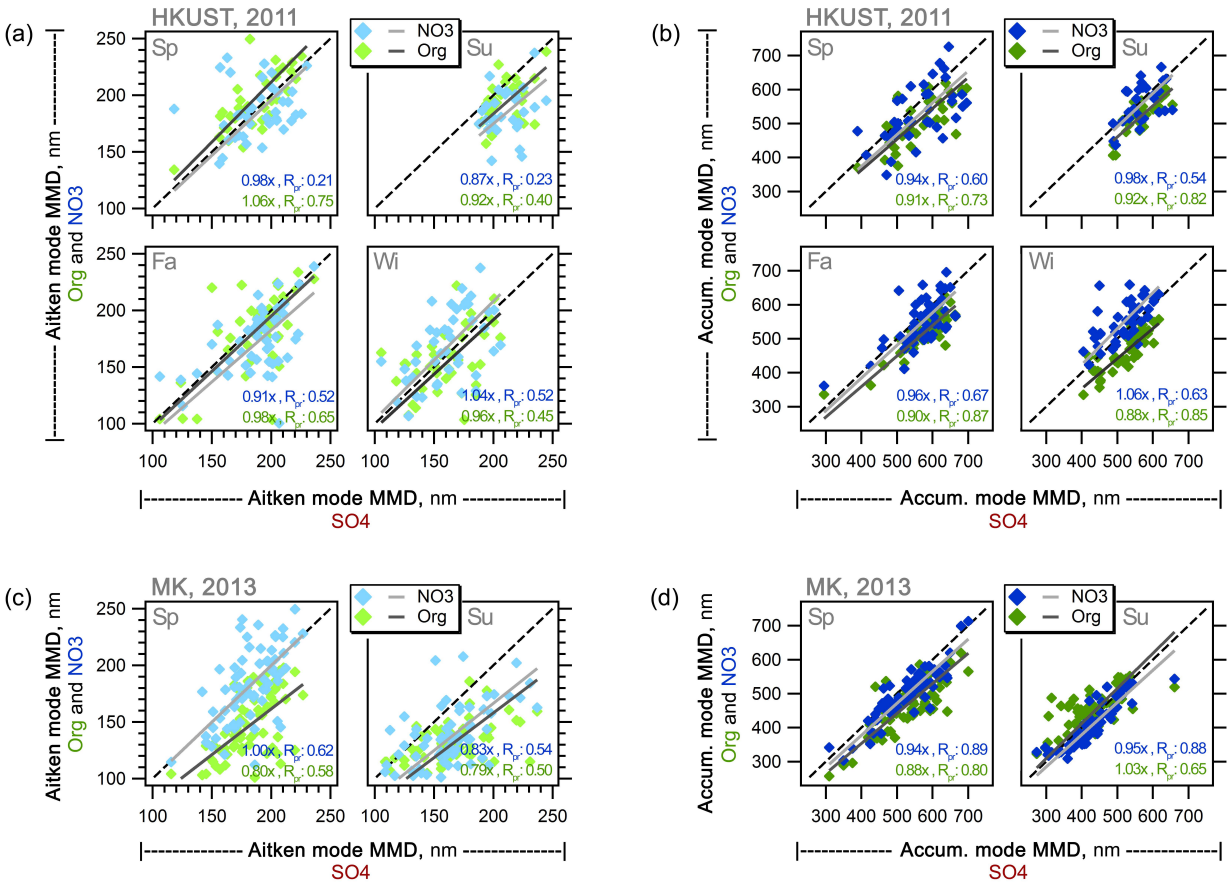

Figure 6. Scatter plots of fitted mass median diameters of organics and nitrate vs. sulfate for the (a) Aitken mode and (b) accumulation mode at the HKUST suburban site, and (c) Aitken mode and (d) accumulation mode at the urban Mong Kok site

3.3. Comparison to previous studies

Particle size distribution studies in Hong Kong are generally scarce and have focused on either size segregated filter samples (MOUDI) for general ambient measurements or electrostatic classification in particle formation and particle growth studies (Guo et al., 2012;Cheung et al., 2015) . The latter studies focus on specific and narrow time periods and lack general discussions on ambient particle size distributions.

Two ambient studies were undertaken at the suburban coastal HKUST site using size-segregated samples from a ten-stage MOUDI sampler and offline chromatographic analysis. Inorganic constituents (NH4, NO3, SO4) in fine particles (i.e. D_p<1.8 µm) were shown to follow bimodal distributions with mode diameters in the range of 0.14-0.21 µm and 0.46-0.58 µm in samples collected in the winter season, while the main mode was observed in the coarse region (4-6 µm) for all three species (Zhuang et al., 1999). A subsequent year-long observational study also reported bimodal fine particle distributions with mode diameters of 0.1-0.3 µm and 0.7–0.9 µm and 1-2 additional modes in the coarse region (Bian et al., 2014), however, the main mode in the size distributions of sulfate, ammonium, potassium and oxalate was observed in the droplet mode (0.7 – 0.9 µm) in this study. Vehicle exhaust plumes sampled on-road from a Mobile Real-time Air Monitoring Platform (MAP) across Hong Kong's road network exhibited three distinct particle volume size distributions: a unimodal distribution with an accumulation mode at 0.2 µm and two bimodal distributions with a minor mode at 0.2 µm and the dominant mode at 0.5 or 0.7 µm (Yao et al., 2007a).

The bimodality in the fine particle range across these studies is consistent with the AMS-based results in this work. Nominally, the accumulation mode diameters from filter based studies and the chase studies are larger than those from AMS measurements where maximum mode diameters occurred at D_{va} ~ 700nm, corresponding to D_a ~ 470 (assuming D_{va} ~ D_a * density; particle density ~ 1.5 g/cm^3). Direct comparability is however limited due to fundamental differences in sizing techniques (MOUDI: atmospheric pressure; AMS: near-vacuum), sampling times (MOUDI: 24h samples, scattered time line; AMS: minute raw resolution averaged to hourly or daily, continuous time line), measurement uncertainties (MOUDI: sampling artifacts such as vapor adsorption and desorption; AMS: inlet lens transmission) and aerosol pretreatment (none for MOUDI with potential impacts on particle size in high humidity (>80%) conditions (Fang et al., 1991); AMS: removal of water prior to introduction to instrument).

3.4. Influence of AMS lens transmission

The quantitative measurement of particle components in the AMS is dependent on three major factors which may lead to particle loss prior to detection (Huffman et al., 2005). Irregularly shaped particles deviating from the flight path in the vacuum chamber may miss the vaporizer. Particles bouncing off the vaporizer surface will not be vaporized and hence may not be detected. Lastly, the aerodynamic lens which is part of the instrument's inlet system does not transmit particles uniformly across all particle diameters. Small particles are lost due to insufficient focusing or diffusion and large particle impact the lens apertures (Liu et al., 2007;Williams et al., 2013). Being a function of particle size, the latter factor affects both total AMS quantifiable particle mass (NR-PM_1) and measured mass size distributions. Transmission curves determined for the standard lens, which is fitted in most AMS instruments, can

vary but typically show efficient (i.e. close to 100%) transmission in the range of 100-550nm (Knote et al., 2011) falling of significantly at either edge.

We examined the potential impact of lens transmission on the AMS mass size distributions on a number of 24h size distributions from the fall season HKUST dataset covering both efficient and reduced lens transmission size regimes (accumulation mode diameters between 400 and 600nm). Panels a-c in Figure D18 in the Supporting Material depict original and lens-transmission corrected 24h mass size distributions for organic, nitrate and sulfate, assuming the transmission function (subpanel d) reported by Liu et al., 2007. Impacts were generally larger in the accumulation mode range with evident shifts to larger mode diameters and larger mode mass concentrations observed in all size distributions. In the small diameter range, enhanced shoulders can occur which may however be artifacts due to the larger uncertainties (low signal to noise ratio at small particle mass), i.e. greater noisiness at the leading end of AMS size distributions. For a quantitative comparison, bimodal fitting parameters from the corrected distributions were plotted against those from, the original distributions in Figure D18 in the Supporting Material (subpanels e-g refer to the Aitken mode and subpanels h-j to the accumulation mode). Leading edge shoulders in the corrected size distributions were not considered in the fitting. Changes in the Aitken mode mass median diameters were minor (on average ~3%), while the integrated mode particle mass increased moderately (~48%). In the accumulation mode, mass median diameters increased by ~28% and integrated mode particle mass doubled. The distribution widths (geometric standard deviations) exhibited little change in both modes (increases of 2-3%).

Fitting results will therefore vary depending on whether AMS size distribution and concentration data are corrected for lens transmission. While explicit lens transmission corrections can improve the accuracy of quantification of AMS species concentration and size distribution measurements, few ambient studies explicitly use lens transmission corrections based on individual experimental determinations or literature values e.g. (Quinn et al., 2006;Cross et al., 2007). Lens transmission curves can vary between instruments (Fast et al., 2009) and are inherently difficult to determine accurately experimentally. As discussed previously, scaling of size distributions by lens transmission curves may introduce artifacts in noisier size distributions (e.g. low end of the Aitken mode, low concentration periods, short term size distribution averages). Trailing edges from slow vaporization (e.g. under high particle mass loadings) may be exacerbated and inflate mass concentrations at the upper size cut range of the AMS. The majority of ambient studies employs a combined correction factor (collection efficiency, CE) considered to be the joint product of the previously mentioned transmission efficiencies related to particle bounce, beam broadening and lens transmission (Middlebrook et al., 2012) derived from aerosol composition and by comparison to collocated speciation or particle sizing instruments. As the AMS lens transmission curve could not be determined in this study and to avoid additional uncertainties from the application of non-instrument specific lens transmission values, we followed the CE correction method in the analysis of the size distribution data in this study. The reported values of resolved mode diameters and integrated mode should therefore be regarded as lower bound estimates in the context of the instrumental limitations affecting ambient AMS measurements.

4. Conclusion

A detailed analysis of AMS mass-based particle size distributions of sulfate, nitrate, and organics in submicron particulate matter measured at two contrasting locations in Hong Kong during two field campaigns has been undertaken. Deconvolution of size distributions into Aitken and accumulation submodes was accomplished by log-normal peak fitting and trends in particle size (mass median diameters), dispersity (geometric standard deviation) and overall particle mass (integrated mode area) were discussed on a diurnal time scale and on a daily basis to evaluate longer-term changes in size distribution characteristics. At the urban roadside location, clear diurnal influences of primary particle and gas-phase species were evident affecting both inorganic and organic component size distributions. Traffic and cooking contributed an estimated 0.3 – 0.9 μg/m^3 and 0.5 – 1.8 μg/m^3 of organic component particle mass in the Aitken mode, and 1.6 - 1.8 μg/m^3 and 1.0 – 2.7 μg/m^3 respectively in the accumulation mode with concentrations level varying with seasons. Notable changes in Aitken mode mass median diameters of organics were limited to the morning rush hour. Daytime particle concentration maxima of sulfate and nitrate in summer indicated substantial influence of photochemical processes, which also led to increments in mass median diameters in the accumulation mode thus inferring associated particle growth. Nocturnal nitrate formation was apparent in the accumulation mode in spring concurring with the nighttime peak of ozone at the roadside, while in the Aitken mode nitrate particle concentrations were significantly elevated during the dinner hours. Organics-related size distributions were mostly governed by intra-day changes at the urban site with very similar trends across different size distribution sets (i.e. concentration regimes), while disparities in diurnal variations among different size distribution sets were evident for nitrate and sulfate, particularly affecting the average sets, indicating stronger influence of irregular external factors which were not associated with diurnal time scale processes.

Suburban particle size distributions exhibited variable diurnal characteristics, suggesting that irregular processes such as transport and seasonal meteorological conditions were the more dominant processes influencing particle size characteristics. Aitken mode particle mass of organics was significantly larger in spring and summer indicating greater influence of more local formation sources in the warm season. In the accumulation mode, organic particle mass concentrations were highest in fall and lowest in spring, following the frequency pattern of continental air mass influence. For sulfate, Aitken mode mass concentrations mass concentrations peaked in the afternoon from spring throughout fall with highest nominal concentrations in spring and summer and lowest levels in winter, while accumulation mode particle mass was highest in summer and fall and lowest in winter, similar to the trend observed among organic constituents.

Nitrate particle mass in the Aitken mode was generally small in most seasons (0.01 - 0.06 μg/m^3), except winter where daytime concentrations reached ~0.1 μg/m^3. In both modes, changes in mass median diameters varied temporally and in magnitude with seasons, indicating a stronger influence of specific meteorological conditions on the properties of nitrate-containing particles at the suburban site. At the urban site, periods of greater inorganic species mass concentrations were more likely to be caused by increases in both Aitken and accumulation mode particle mass in summer, indicating that particle formation and growth affecting smaller particles was more likely to occur in the warmer season. At the suburban receptor location, significant correlation of submode particle mass to total species concentration ($0.5 \leq R_{pr} \leq 0.7$) was observed for organics and nitrate in most seasons (spring, summer, winter)

suggesting notable influence of local or regional formation processes on organic and nitrate Aitken mode particulate mass. Variations in particle mixing state were examined by evaluation of inter-species mass median diameter trends at both measurement sites. In the accumulation mode at the urban site, internal mixing appeared to be prevalent in spring, while greater frequency of time periods with external mixing of particle populations comprising different fractions of organic constituents was observed in summer. External mixing was predominant in the Aitken mode at the urban location in both seasons. At the suburban site, sulfate and nitrate in the accumulation mode more frequently exhibited differing particle size distributions in all seasons signifying a greater extent of external mixing. In winter, external mixing of more organics enriched particles in the lower accumulation size range was evident.

Acknowledgements

This work was supported by the Environmental Conservation Fund of Hong Kong (project number ECWW09EG04). Chak K. Chan gratefully acknowledges the startup fund of the City University of Hong Kong.

References

Abbatt, J. P. D., Broekhuizen, K., and Pradeep Kumar, P.: Cloud condensation nucleus activity of internally mixed ammonium sulfate/organic acid aerosol particles, Atmospheric Environment, 39, 4767-4778, 10.1016/j.atmosenv.2005.04.029, 2005.

Ahlquist, N. C., and Charlson, R. J.: A New Instrument for Evaluating the Visual Quality of Air, Journal of the Air Pollution Control Association, 17, 467-469, 10.1080/00022470.1967.10469006, 1967.

Aiken, A. C., Salcedo, D., Cubison, M. J., Huffman, J. A., DeCarlo, P. F., Ulbrich, I. M., Docherty, K. S., Sueper, D., Kimmel, J. R., Worsnop, D. R., Trimborn, A., Northway, M., Stone, E. A., Schauer, J. J., Volkamer, R. M., Fortner, E., de Foy, B., Wang, J., Laskin, A., Shutthanandan, V., Zheng, J., Zhang, R., Gaffney, J., Marley, N. A., Paredes-Miranda, G., Arnott, W. P., Molina, L. T., Sosa, G., and Jimenez, J. L.: Mexico City aerosol analysis during MILAGRO using high resolution aerosol mass spectrometry at the urban supersite (T0) - Part 1: Fine particle composition and organic source apportionment, Atmospheric Chemistry and Physics, 9, 6633-6653, 2009.

Bahreini, R., Dunlea, E. J., Matthew, B. M., Simons, C., Docherty, K. S., DeCarlo, P. F., Jimenez, J. L., Brock, C. A., and Middlebrook, A. M.: Design and Operation of a Pressure-Controlled Inlet for Airborne Sampling with an Aerodynamic Aerosol Lens, Aerosol Science and Technology, 42, 465-471, 10.1080/02786820802178514, 2008.

Bian, Q., Huang, X. H. H., and Yu, J. Z.: One-year observations of size distribution characteristics of major aerosol constituents at a coastal receptor site in Hong Kong – Part 1: Inorganic ions and oxalate, Atmos. Chem. Phys., 14, 9013-9027, 10.5194/acp-14-9013-2014, 2014.

Bohren, C. F., and Huffman, D. R.: Absorption and scattering of light by small particles, in: Absorption and Scattering of Light by Small Particles, Wiley-VCH Verlag GmbH, 1-11, 1983.

735 Canagaratna, M. R., Jayne, J. T., Jimenez, J. L., Allan, J. D., Alfarra, M. R., Zhang, Q., Onasch, T. B., Drewnick, F.,
736 Coe, H., Middlebrook, A., Delia, A., Williams, L. R., Trimborn, A. M., Northway, M. J., DeCarlo, P. F., Kolb,
737 C. E., Davidovits, P., and Worsnop, D. R.: Chemical and microphysical characterization of ambient aerosols
738 with the aerodyne aerosol mass spectrometer, Mass Spectrometry Reviews, 26, 185-222, 10.1002/mas.20115,
739 2007.
740 Charlson, R. J., Langner, J., Rodhe, H., Leovy, C. B., and Warren, S. G.: Perturbation of the northern hemisphere
741 radiative balance by backscattering from anthropogenic sulfate aerosols*, Tellus B, 43, 152-163,
742 10.1034/j.1600-0889.1991.t01-1-00013.x, 1991.
743 Cheung, K., Ling, Z. H., Wang, D. W., Wang, Y., Guo, H., Lee, B., Li, Y. J., and Chan, C. K.: Characterization and
744 source identification of sub-micron particles at the HKUST Supersite in Hong Kong, Science of The Total
745 Environment, 527–528, 287-296, http://dx.doi.org/10.1016/j.scitotenv.2015.04.087, 2015.
746 Crippa, M., DeCarlo, P. F., Slowik, J. G., Mohr, C., Heringa, M. F., Chirico, R., Poulain, L., Freutel, F., Sciare, J.,
747 Cozic, J., Di Marco, C. F., Elsasser, M., Nicolas, J. B., Marchand, N., Abidi, E., Wiedensohler, A., Drewnick,
748 F., Schneider, J., Borrmann, S., Nemitz, E., Zimmermann, R., Jaffrezo, J. L., Prévôt, A. S. H., and
749 Baltensperger, U.: Wintertime aerosol chemical composition and source apportionment of the organic fraction
750 in the metropolitan area of Paris, Atmos. Chem. Phys., 13, 961-981, 10.5194/acp-13-961-2013, 2013.
751 Cross, E. S., Slowik, J. G., Davidovits, P., Allan, J. D., Worsnop, D. R., Jayne, J. T., Lewis †, D. K., Canagaratna,
752 M., and Onasch, T. B.: Laboratory and Ambient Particle Density Determinations using Light Scattering in
753 Conjunction with Aerosol Mass Spectrometry, Aerosol Science and Technology, 41, 343-359,
754 10.1080/02786820701199736, 2007.
755 Cross, E. S., Onasch, T. B., Canagaratna, M., Jayne, J. T., Kimmel, J., Yu, X. Y., Alexander, M. L., Worsnop, D. R.,
756 and Davidovits, P.: Single particle characterization using a light scattering module coupled to a time-of-flight
757 aerosol mass spectrometer, Atmos. Chem. Phys., 9, 7769-7793, 10.5194/acp-9-7769-2009, 2009.
758 Davidson, C. I., Phalen, R. F., and Solomon, P. A.: Airborne Particulate Matter and Human Health: A Review,
759 Aerosol Science and Technology, 39, 737-749, 10.1080/02786820500191348, 2005.
760 DeCarlo, P. F., Slowik, J. G., Worsnop, D. R., Davidovits, P., and Jimenez, J. L.: Particle morphology and density
761 characterization by combined mobility and aerodynamic diameter measurements. Part 1: Theory, Aerosol
762 Science and Technology, 38, 1185-1205, 10.1080/027868290903907, 2004.
763 Docherty, K. S., Aiken, A. C., Huffman, J. A., Ulbrich, I. M., DeCarlo, P. F., Sueper, D., Worsnop, D. R., Snyder,
764 D. C., Peltier, R. E., Weber, R. J., Grover, B. D., Eatough, D. J., Williams, B. J., Goldstein, A. H., Ziemann, P.
765 J., and Jimenez, J. L.: The 2005 Study of Organic Aerosols at Riverside (SOAR-1): instrumental
766 intercomparisons and fine particle composition, Atmospheric Chemistry and Physics, 11, 12387-12420,
767 10.5194/acp-11-12387-2011, 2011.
768 Docherty, K. S., Lewandowski, M., and Jimenez, J. L.: Effect of Vaporizer Temperature on Ambient Non-
769 Refractory Submicron Aerosol Composition and Mass Spectra Measured by the Aerosol Mass Spectrometer,
770 Aerosol Science and Technology, 49, 485-494, 10.1080/02786826.2015.1042100, 2015.

771 Drewnick, F., Hings, S. S., DeCarlo, P., Jayne, J. T., Gonin, M., Fuhrer, K., Weimer, S., Jimenez, J. L., Demerjian,
772 K. L., Borrmann, S., and Worsnop, D. R.: A new time-of-flight aerosol mass spectrometer (TOF-AMS) -
773 Instrument description and first field deployment, Aerosol Science and Technology, 39, 637-658,
774 10.1080/02786820500182040, 2005.
775 Elser, M., Huang, R. J., Wolf, R., Slowik, J. G., Wang, Q., Canonaco, F., Li, G., Bozzetti, C., Daellenbach, K. R.,
776 Huang, Y., Zhang, R., Li, Z., Cao, J., Baltensperger, U., El-Haddad, I., and Prévôt, A. S. H.: New insights into
777 PM2.5 chemical composition and sources in two major cities in China during extreme haze events using aerosol
778 mass spectrometry, Atmos. Chem. Phys., 16, 3207-3225, 10.5194/acp-16-3207-2016, 2016.
779 Farmer, D. K., Matsunaga, A., Docherty, K. S., Surratt, J. D., Seinfeld, J. H., Ziemann, P. J., and Jimenez, J. L.:
780 Response of an aerosol mass spectrometer to organonitrates and organosulfates and implications for
781 atmospheric chemistry, Proceedings of the National Academy of Sciences of the United States of America, 107,
782 6670-6675, 10.1073/pnas.0912340107, 2010.
783 Fast, J., Aiken, A. C., Allan, J., Alexander, L., Campos, T., Canagaratna, M. R., Chapman, E., DeCarlo, P. F., de
784 Foy, B., Gaffney, J., de Gouw, J., Doran, J. C., Emmons, L., Hodzic, A., Herndon, S. C., Huey, G., Jayne, J. T.,
785 Jimenez, J. L., Kleinman, L., Kuster, W., Marley, N., Russell, L., Ochoa, C., Onasch, T. B., Pekour, M., Song,
786 C., Ulbrich, I. M., Warneke, C., Welsh-Bon, D., Wiedinmyer, C., Worsnop, D. R., Yu, X. Y., and Zaveri, R.:
787 Evaluating simulated primary anthropogenic and biomass burning organic aerosols during MILAGRO:
788 implications for assessing treatments of secondary organic aerosols, Atmospheric Chemistry and Physics, 9,
789 6191-6215, 2009.
790 Gill, P. E., Murray, W., and Wright, M. H.: The Levenberg-Marquardt method, in: Practical optimization, Academic
791 Press, London, 1981.
792 Griffith, S. M., Huang, X. H. H., Louie, P. K. K., and Yu, J. Z.: Characterizing the thermodynamic and chemical
793 composition factors controlling PM2.5 nitrate: Insights gained from two years of online measurements in Hong
794 Kong, Atmospheric Environment, 122, 864-875, http://dx.doi.org/10.1016/j.atmosenv.2015.02.009, 2015.
795 Guo, H., Wang, D. W., Cheung, K., Ling, Z. H., Chan, C. K., and Yao, X. H.: Observation of aerosol size
796 distribution and new particle formation at a mountain site in subtropical Hong Kong, Atmos. Chem. Phys., 12,
797 9923-9939, 10.5194/acp-12-9923-2012, 2012.
798 Huang, X. F., He, L. Y., Hu, M., Canagaratna, M. R., Sun, Y., Zhang, Q., Zhu, T., Xue, L., Zeng, L. W., Liu, X. G.,
799 Zhang, Y. H., Jayne, J. T., Ng, N. L., and Worsnop, D. R.: Highly time-resolved chemical characterization of
800 atmospheric submicron particles during 2008 Beijing Olympic Games using an Aerodyne High-Resolution
801 Aerosol Mass Spectrometer, Atmospheric Chemistry and Physics, 10, 8933-8945, 10.5194/acp-10-8933-2010,
802 2010.
803 Huang, X. F., He, L. Y., Hu, M., Canagaratna, M. R., Kroll, J. H., Ng, N. L., Zhang, Y. H., Lin, Y., Xue, L., Sun, T.
804 L., Liu, X. G., Shao, M., Jayne, J. T., and Worsnop, D. R.: Characterization of submicron aerosols at a rural site
805 in Pearl River Delta of China using an Aerodyne High-Resolution Aerosol Mass Spectrometer, Atmospheric
806 Chemistry and Physics, 11, 1865-1877, 10.5194/acp-11-1865-2011, 2011.

807 Huang, X. H. H., Bian., Q. J., Ng, W. M., Louie, P. K. K., and Yu, J. Z.: Characterization of PM2.5 Major
808 Components and Source Investigation in Suburban Hong Kong: A One Year Monitoring Study, Aerosol and Air
809 Quality Research 14, 237-250, 2014.
810 Huffman, J. A., Jayne, J. T., Drewnick, F., Aiken, A. C., Onasch, T., Worsnop, D. R., and Jimenez, J. L.: Design,
811 modeling, optimization, and experimental tests of a particle beam width probe for the aerodyne aerosol mass
812 spectrometer, Aerosol Science and Technology, 39, 1143-1163, 10.1080/02786820500423782, 2005.
813 Jayne, J. T., Leard, D. C., Zhang, X. F., Davidovits, P., Smith, K. A., Kolb, C. E., and Worsnop, D. R.:
814 Development of an aerosol mass spectrometer for size and composition analysis of submicron particles, Aerosol
815 Science and Technology, 33, 49-70, 2000.
816 Jimenez, J. L., Jayne, J. T., Shi, Q., Kolb, C. E., Worsnop, D. R., Yourshaw, I., Seinfeld, J. H., Flagan, R. C., Zhang,
817 X., Smith, K. A., Morris, J. W., and Davidovits, P.: Ambient aerosol sampling using the Aerodyne Aerosol
818 Mass Spectrometer, J. Geophys. Res., 108, 8425, 10.1029/2001jd001213, 2003.
819 John, W.: Size Distribution Characteristics of Aerosols, in: Aerosol Measurement, John Wiley & Sons, Inc., 41-54,
820 2011.
821 Kerminen, V. M., Paramonov, M., Anttila, T., Riipinen, I., Fountoukis, C., Korhonen, H., Asmi, E., Laakso, L.,
822 Lihavainen, H., Swietlicki, E., Svenningsson, B., Asmi, A., Pandis, S. N., Kulmala, M., and Petäjä, T.: Cloud
823 condensation nuclei production associated with atmospheric nucleation: a synthesis based on existing literature
824 and new results, Atmos. Chem. Phys., 12, 12037-12059, 10.5194/acp-12-12037-2012, 2012.
825 Knote, C., Brunner, D., Vogel, H., Allan, J., Asmi, A., Äijälä, M., Carbone, S., van der Gon, H. D., Jimenez, J. L.,
826 Kiendler-Scharr, A., Mohr, C., Poulain, L., Prévôt, A. S. H., Swietlicki, E., and Vogel, B.: Towards an online-
827 coupled chemistry-climate model: evaluation of trace gases and aerosols in COSMO-ART, Geosci. Model Dev.,
828 4, 1077-1102, 10.5194/gmd-4-1077-2011, 2011.
829 Köhler, H.: The nucleus in and the growth of hygroscopic droplets, Transactions of the Faraday Society, 32, 1152-
830 1161, 10.1039/tf9363201152, 1936.
831 Lee, B. P., Li, Y. J., Yu, J. Z., Louie, P. K. K., and Chan, C. K.: Physical and chemical characterization of ambient
832 aerosol by HR-ToF-AMS at a suburban site in Hong Kong during springtime 2011, Journal of Geophysical
833 Research: Atmospheres, 118, 8625-8639, 10.1002/jgrd.50658, 2013.
834 Lee, B. P., Li, Y. J., Yu, J. Z., Louie, P. K. K., and Chan, C. K.: Characteristics of submicron particulate matter at
835 the urban roadside in downtown Hong Kong—Overview of 4 months of continuous high-resolution aerosol
836 mass spectrometer measurements, Journal of Geophysical Research: Atmospheres, 120, 7040-7058,
837 10.1002/2015JD023311, 2015.
838 Li, Y. J., Lee, B. Y. L., Yu, J. Z., Ng, N. L., and Chan, C. K.: Evaluating the degree of oxygenation of organic
839 aerosol during foggy and hazy days in Hong Kong using high-resolution time-of-flight aerosol mass
840 spectrometry (HR-ToF-AMS), Atmos. Chem. Phys., 13, 8739-8753, 10.5194/acp-13-8739-2013, 2013.
841 Li, Y. J., Lee, B. P., Su, L., Fung, J. C. H., and Chan, C. K.: Seasonal characteristics of fine particulate matter (PM)
842 based on high resolution time-of-flight aerosol mass spectrometric (HR-ToF-AMS) measurements at the
843 HKUST Supersite in Hong Kong, Atmos. Chem. Phys., 15, 37-53, doi:10.5194/acp-15-37-2015, 2015.

Liu, P. S. K., Deng, R., Smith, K. A., Williams, L. R., Jayne, J. T., Canagaratna, M. R., Moore, K., Onasch, T. B., Worsnop, D. R., and Deshler, T.: Transmission efficiency of an aerodynamic focusing lens system: Comparison of model calculations and laboratory measurements for the Aerodyne Aerosol Mass Spectrometer, Aerosol Science and Technology, 41, 721-733, 10.1080/02786820701422278, 2007.

Man, H., Zhu, Y., Ji, F., Yao, X., Lau, N. T., Li, Y., Lee, B. P., and Chan, C. K.: Comparison of Daytime and Nighttime New Particle Growth at the HKUST Supersite in Hong Kong, Environmental Science & Technology, 49, 7170-7178, 10.1021/acs.est.5b02143, 2015.

Meng, J. W., Yeung, M. C., Li, Y. J., Lee, B. Y. L., and Chan, C. K.: Size-resolved cloud condensation nuclei (CCN) activity and closure analysis at the HKUST Supersite in Hong Kong, Atmos. Chem. Phys., 14, 10267-10282, 10.5194/acp-14-10267-2014, 2014.

Middlebrook, A. M., Bahreini, R., Jimenez, J. L., and Canagaratna, M. R.: Evaluation of Composition-Dependent Collection Efficiencies for the Aerodyne Aerosol Mass Spectrometer using Field Data, Aerosol Science and Technology, 46, 258-271, 10.1080/02786826.2011.620041, 2012.

Mohr, C., DeCarlo, P. F., Heringa, M. F., Chirico, R., Slowik, J. G., Richter, R., Reche, C., Alastuey, A., Querol, X., Seco, R., Peñuelas, J., Jiménez, J. L., Crippa, M., Zimmermann, R., Baltensperger, U., and Prévôt, A. S. H.: Identification and quantification of organic aerosol from cooking and other sources in Barcelona using aerosol mass spectrometer data, Atmos. Chem. Phys., 12, 1649-1665, 10.5194/acp-12-1649-2012, 2012.

Quinn, P. K., Bates, T. S., Coffman, D., Onasch, T. B., Worsnop, D., Baynard, T., de Gouw, J. A., Goldan, P. D., Kuster, W. C., Williams, E., Roberts, J. M., Lerner, B., Stohl, A., Pettersson, A., and Lovejoy, E. R.: Impacts of sources and aging on submicrometer aerosol properties in the marine boundary layer across the Gulf of Maine, J. Geophys. Res., 111, D23S36, 10.1029/2006jd007582, 2006.

Rupakheti, M., Leaitch, W. R., Lohmann, U., Hayden, K., Brickell, P., Lu, G., Li, S. M., Toom-Sauntry, D., Bottenheim, J. W., Brook, J. R., Vet, R., Jayne, J. T., and Worsnop, D. R.: An intensive study of the size and composition of submicron atmospheric aerosols at a rural site in Ontario, Canada, Aerosol Science and Technology, 39, 722-736, 10.1080/02786820500182420, 2005.

Saarikoski, S., Carbone, S., Decesari, S., Giulianelli, L., Angelini, F., Canagaratna, M., Ng, N. L., Trimborn, A., Facchini, M. C., Fuzzi, S., Hillamo, R., and Worsnop, D.: Chemical characterization of springtime submicrometer aerosol in Po Valley, Italy, Atmos. Chem. Phys., 12, 8401-8421, 10.5194/acp-12-8401-2012, 2012.

Salcedo, D., Onasch, T. B., Dzepina, K., Canagaratna, M. R., Zhang, Q., Huffman, J. A., DeCarlo, P. F., Jayne, J. T., Mortimer, P., Worsnop, D. R., Kolb, C. E., Johnson, K. S., Zuberi, B., Marr, L. C., Volkamer, R., Molina, L. T., Molina, M. J., Cardenas, B., Bernabe, R. M., Marquez, C., Gaffney, J. S., Marley, N. A., Laskin, A., Shutthanandan, V., Xie, Y., Brune, W., Lesher, R., Shirley, T., and Jimenez, J. L.: Characterization of ambient aerosols in Mexico City during the MCMA-2003 campaign with Aerosol Mass Spectrometry: results from the CENICA Supersite, Atmospheric Chemistry and Physics, 6, 925-946, 2006.

Schwartz, S. E.: The whitehouse effect—Shortwave radiative forcing of climate by anthropogenic aerosols: an overview, Journal of Aerosol Science, 27, 359-382, http://dx.doi.org/10.1016/0021-8502(95)00533-1, 1996.

881 Seinfeld, J. H., and Pandis, S. N.: Atmospheric Chemistry and Physics - From Air Pollution to Climate Change (2nd
882 Edition). John Wiley & Sons, 2006.
883 Setyan, A., Zhang, Q., Merkel, M., Knighton, W. B., Sun, Y., Song, C., Shilling, J. E., Onasch, T. B., Herndon, S.
884 C., Worsnop, D. R., Fast, J. D., Zaveri, R. A., Berg, L. K., Wiedensohler, A., Flowers, B. A., Dubey, M. K., and
885 Subramanian, R.: Characterization of submicron particles influenced by mixed biogenic and anthropogenic
886 emissions using high-resolution aerosol mass spectrometry: results from CARES, Atmos. Chem. Phys., 12,
887 8131-8156, 10.5194/acp-12-8131-2012, 2012.
888 Slowik, J. G., Stainken, K., Davidovits, P., Williams, L. R., Jayne, J. T., Kolb, C. E., Worsnop, D. R., Rudich, Y.,
889 DeCarlo, P. F., and Jimenez, J. L.: Particle morphology and density characterization by combined mobility and
890 aerodynamic diameter measurements. Part 2: Application to combustion-generated soot aerosols as a function of
891 fuel equivalence ratio, Aerosol Science and Technology, 38, 1206-1222, 10.1080/027868290903916, 2004.
892 Sun, C., Lee, B. P., Huang, D., Jie Li, Y., Schurman, M. I., Louie, P. K. K., Luk, C., and Chan, C. K.: Continuous
893 measurements at the urban roadside in an Asian megacity by Aerosol Chemical Speciation Monitor (ACSM):
894 particulate matter characteristics during fall and winter seasons in Hong Kong, Atmos. Chem. Phys., 16, 1713-
895 1728, 10.5194/acp-16-1713-2016, 2016.
896 Sun, Y., Zhang, Q., Macdonald, A. M., Hayden, K., Li, S. M., Liggio, J., Liu, P. S. K., Anlauf, K. G., Leaitch, W.
897 R., Steffen, A., Cubison, M., Worsnop, D. R., van Donkelaar, A., and Martin, R. V.: Size-resolved aerosol
898 chemistry on Whistler Mountain, Canada with a high-resolution aerosol mass spectrometer during INTEX-B,
899 Atmos. Chem. Phys., 9, 3095-3111, 10.5194/acp-9-3095-2009, 2009.
900 Sun, Y. L., Zhang, Q., Schwab, J. J., Demerjian, K. L., Chen, W. N., Bae, M. S., Hung, H. M., Hogrefe, O., Frank,
901 B., Rattigan, O. V., and Lin, Y. C.: Characterization of the sources and processes of organic and inorganic
902 aerosols in New York city with a high-resolution time-of-flight aerosol mass apectrometer, Atmospheric
903 Chemistry and Physics, 11, 1581-1602, 10.5194/acp-11-1581-2011, 2011.
904 Takegawa, N., Miyakawa, T., Watanabe, M., Kondo, Y., Miyazaki, Y., Han, S., Zhao, Y., van Pinxteren, D.,
905 Bruggemann, E., Gnauk, T., Herrmann, H., Xiao, R., Deng, Z., Hu, M., Zhu, T., and Zhang, Y.: Performance of
906 an Aerodyne Aerosol Mass Spectrometer (AMS) during Intensive Campaigns in China in the Summer of 2006,
907 Aerosol Science and Technology, 43, 189-204, 10.1080/02786820802582251, 2009.
908 Ulbrich, I. M., Canagaratna, M. R., Cubison, M. J., Zhang, Q., Ng, N. L., Aiken, A. C., and Jimenez, J. L.: Three-
909 dimensional factorization of size-resolved organic aerosol mass spectra from Mexico City, Atmos. Meas. Tech.,
910 5, 195-224, 10.5194/amt-5-195-2012, 2012.
911 Westervelt, D. M., Pierce, J. R., Riipinen, I., Trivitayanurak, W., Hamed, A., Kulmala, M., Laaksonen, A., Decesari,
912 S., and Adams, P. J.: Formation and growth of nucleated particles into cloud condensation nuclei: model–
913 measurement comparison, Atmos. Chem. Phys., 13, 7645-7663, 10.5194/acp-13-7645-2013, 2013.
914 Williams, L. R., Gonzalez, L. A., Peck, J., Trimborn, D., McInnis, J., Farrar, M. R., Moore, K. D., Jayne, J. T.,
915 Robinson, W. A., Lewis, D. K., Onasch, T. B., Canagaratna, M. R., Trimborn, A., Timko, M. T., Magoon, G.,
916 Deng, R., Tang, D., de la Rosa Blanco, E., Prévôt, A. S. H., Smith, K. A., and Worsnop, D. R.: Characterization

of an aerodynamic lens for transmitting particles greater than 1 micrometer in diameter into the Aerodyne aerosol mass spectrometer, Atmos. Meas. Tech., 6, 3271-3280, 10.5194/amt-6-3271-2013, 2013.

Yao, X., Lau, N. T., Chan, C. K., and Fang, M.: Size distributions and condensation growth of submicron particles in on-road vehicle plumes in Hong Kong, Atmospheric Environment, 41, 3328-3338, 10.1016/j.atmosenv.2006.12.044, 2007a.

Yao, X., Ling, T. Y., Fang, M., and Chan, C. K.: Size dependence of in situ pH in submicron atmospheric particles in Hong Kong, Atmospheric Environment, 41, 382-393, 10.1016/j.atmosenv.2006.07.037, 2007b.

Yuan, Z., Yadav, V., Turner, J. R., Louie, P. K. K., and Lau, A. K. H.: Long-term trends of ambient particulate matter emission source contributions and the accountability of control strategies in Hong Kong over 1998–2008, Atmospheric Environment, 76, 21-31, http://dx.doi.org/10.1016/j.atmosenv.2012.09.026, 2013.

Zhang, J. K., Sun, Y., Liu, Z. R., Ji, D. S., Hu, B., Liu, Q., and Wang, Y. S.: Characterization of submicron aerosols during a month of serious pollution in Beijing, 2013, Atmos. Chem. Phys., 14, 2887-2903, 10.5194/acp-14-2887-2014, 2014.

Zhang, Q., Stanier, C. O., Canagaratna, M. R., Jayne, J. T., Worsnop, D. R., Pandis, S. N., and Jimenez, J. L.: Insights into the chemistry of new particle formation and growth events in Pittsburgh based on aerosol mass spectrometry, Environmental Science & Technology, 38, 4797-4809, 10.1021/es035417u, 2004.

Zhang, Q., Canagaratna, M. R., Jayne, J. T., Worsnop, D. R., and Jimenez, J. L.: Time- and size-resolved chemical composition of submicron particles in Pittsburgh: Implications for aerosol sources and processes, Journal of Geophysical Research-Atmospheres, 110, D07s09 Artn d07s09, 2005.

Zheng, M., Kester, D. R., Wang, F., Shi, X., and Guo, Z.: Size distribution of organic and inorganic species in Hong Kong aerosols during the wet and dry seasons, J. Geophys. Res., 113, D16303, 10.1029/2007jd009494, 2008.

Zhuang, H., Chan, C. K., Fang, M., and Wexler, A. S.: Size distributions of particulate sulfate, nitrate, and ammonium at a coastal site in Hong Kong, Atmospheric Environment, 33, 843-853, 10.1016/s1352-2310(98)00305-7, 1999.